Motor-independent targeting of CLASPs to kinetochores by CENP-E promotes microtubule turnover and poleward flux

Stefano Maffini[1], Ana R. R. Maia[1], Amity L. Manning[2], Zoltan Maliga[3], Ana L. Pereira[1,4], Magno Junqueira[3], Andrej Shevchenko[3], Anthony Hyman[3], John R. Yates III[5], Niels Galjart[4], Duane A. Compton[2], Helder Maiato[1,6]

[1] Instituto de Biologia Molecular e Celular, Universidade do Porto, Rua do Campo Alegre 823, 4150-180 Porto, Portugal

[2] Department of Biochemistry, Dartmouth Medical School, Hanover, NH 03755; Norris Cotton Cancer Center, Dartmouth-Hitchcock Medical Center, Lebanon, NH 03766, USA

[3] Max Planck Institute for Molecular Cell Biology and Genetics, 01307 Dresden, Germany

[4] Department of Cell Biology and Department of Genetics, Erasmus MC Rotterdam, 3000 CA Rotterdam, The Netherlands

[5] The Scripps Research Institute, 10550 North Torrey Pines Rd., SR11, Department of Chemical Physiology, La Jolla, CA 92037, USA

[6] Laboratory of Cell and Molecular Biology, Faculdade de Medicina, Universidade do Porto, 4200-319 Porto, Portugal

Running title: CENP-E targeting of CLASPs to kinetochores

Keywords: Flux; Kinetochore; Microtubule turnover; Mitosis; Mitotic spindle

Abbreviations: KT, kinetochore; MT, microtubule; GFP, green fluorescent protein; LAP, localization affinity purification; SAC, Spindle-assembly checkpoint.

Corresponding Author:

Helder Maiato
Instituto de Biologia Molecular e Celular,
Universidade do Porto
Rua do Campo Alegre, 823
4150-180 Porto
Portugal
Tel: +351 22 607 4900
Fax: +351 22 609 9157
e-mail: maiato@ibmc.up.pt

Summary:

Efficient chromosome segregation during mitosis relies on the coordinated activity of molecular motors with proteins that regulate kinetochore attachments to dynamic spindle microtubules [1]. CLASPs are conserved kinetochore- and microtubule-associated proteins encoded by two paralogue genes, *clasp1* and *clasp2*, and have been previously implicated in the regulation of kinetochore-microtubule dynamics [2-4]. However, it remains unknown how CLASPs work in concert with other proteins to form a functional kinetochore-microtubule interface. Here we have identified mitotic interactors of human CLASP1 using a proteomic approach. Among these, the microtubule plus-end directed motor CENP-E [5] was found to form a complex with CLASP1 that co-localizes to multiple structures of the mitotic apparatus in human cells. We found that CENP-E recruits both CLASP1 and CLASP2 to kinetochores independent of its motor activity or the presence of microtubules. Depletion of CLASPs or CENP-E by RNAi in human cells causes a significant and comparable reduction of kinetochore-microtubule poleward flux and turnover rates, as well as rescues spindle bipolarity in Kif2a-depleted cells. We conclude that CENP-E integrates two critical functions that are important for accurate chromosome movement and spindle architecture: one relying directly on its motor activity and the other involving the targeting of key microtubule regulators to kinetochores.

Results and Discussion

To shed light on the molecular context of human CLASPs during mitosis we identified CLASP1-interacting proteins from nocodazole arrested HeLa cells stably expressing LAP-tagged CLASP1 [4]. LAP purification [6] followed by mass spectrometry analysis recovered known CLASP1 interactors in mammals, such as CLIP-170, LL5β, GCC185 and Astrin [7-9] (Manning et al., submitted). Additionally, we identified CENP-E in our human CLASP1 purification, confirming previous results obtained in *Xenopus* meiotic egg extracts [10]. This approach also identified novel candidate CLASP1 binding partners, including the centriolar proteins CENP-J/CPAP and Ninein [11, 12], as well as MARK kinases [13] (Figure 1a).

From the full list of CLASP1 interactors, (Table S1) CENP-E is the only *bona fide* kinetochore (KT) protein [14]. Importantly, the functional significance of the CLASP1/CENP-E interaction remains unknown and therefore was selected for an in-depth analysis. We started by using mass spectrometry to confirm that endogenous CLASP1 co-purifies with CENP-E (Figure 1a). Notably, endogenous CLASP2 was also found in the purification, suggesting that CENP-E forms distinct complexes with CLASP1 and CLASP2 (Figure 1a). The reciprocal interaction of human CLASP1 with CENP-E was confirmed by Western blot after immunoprecipitation with anti-GFP antibodies in nocodazole arrested HeLa cells stably expressing GFP-CLASP1 or CENP-E-GFP (Figure 1b). Finally, immunofluorescence analysis showed that endogenous CLASP1 and CENP-E co-localize to multiple structures of the mitotic apparatus throughout mitosis, including centrosomes, KTs, spindle mid-zone and mid-body (Figure

S1). Altogether these data suggest that CLASPs and CENP-E may be involved in functionally related aspects of mitosis.

Previous work in *C. elegans*, an organism lacking CENP-E orthologues, has shown that the CENP-F-like proteins HCP-1 and HCP-2 recruit CLASP to KTs [15]. However, as opposed to *C. elegans*, CENP-F depletion in human cells apparently does not affect CLASP1 KT-recruitment [16]. In order to test whether in human cells CENP-E could fulfill the task of targeting CLASPs to KTs, we depleted ~80% of CENP-E from HeLa cells (Figure S2), which led to a significant reduction of CLASP1 (~80%, n Luciferase RNAi=387 KTs from 18 cells; n CENP-E RNAi=579 KTs from 15 cells; $p<0.001$, Mann-Whitney test) and CLASP2 (~65%, n Luciferase RNAi=332 KTs from 10 cells; n CENP-E RNAi=321 KTs from 10 cells; $p<0.001$, Mann-Whitney test) KT levels, in a microtubule (MT)-independent manner (Figure 2a, b and f, Figures S3 and S4). Importantly, CLASP1 and CLASP2 localization in the spindle and centrosomes was not affected by CENP-E depletion (Figure 2b, Figure 3b, and data not shown). On the contrary, depletion of both CLASPs from HeLa cells by RNAi (~90% depletion, Figures S2 and S6) caused no measurable change in CENP-E localization at KTs (n Luciferase RNAi =350 KTs from 9 cells; n CLASPs-RNAi=348 KTs from 8 cells; $p=0.438$, Mann-Whitney test), regardless of the presence of MTs (Figure 2c, and Figures S3 and S6). Under these conditions, CLASP1 was completely removed from KTs, but a detectable RNAi resistant pool of stable protein remained associated with structures at spindle poles resembling centrioles (Figure 2c) [4]. Overall, these results indicate that CENP-E is required to specifically target a very significant pool of CLASP1 and CLASP2 to KTs.

The MT independence of CENP-E-mediated targeting of CLASPs to KTs makes it unlikely to rely on the MT plus-end directed motor activity of CENP-E. To directly test this prediction we quantified CLASP1 KT levels in HeLa cells over-expressing a motor-less CENP-E construct (GFP-CENP-E NΔ803), which causes a dominant-negative effect by preventing endogenous CENP-E from assembling onto KTs [17] and recruits CLASP1 to many cytoplasmic aggregates (Figure S5). Under these conditions, CLASP1 KT levels were similar to non-transfected control cells (Figure 2d and f, n non-transfected= 322 KTs from 8 cells; n transfected=308 KTs from 8 cells). To confirm these results, we used a recently identified fluorenone, UA62784, reported to inhibit CENP-E ATPase activity but not its KT localization [18]. HeLa cells treated with 100 nM of UA62784 for 12 h showed normal CENP-E and CLASP1 localization at KTs (Figure 2e and f and Figure S3; n Control=314 KTs from 8 cells; n UA62784 treated=299 KTs from 8 cells). Overall, these results lead to two conclusions: 1) CENP-E motor domain is not required for interaction with CLASP1; and 2) recruitment of CLASP1 to KTs is a novel motor-independent function of CENP-E.

One remarkable feature of KTs is the capacity of constantly renewing their MT composition (i.e. KT-MT turnover), while allowing the poleward translocation/flux of attached MTs [19]. This is critical to ensure proper chromosome segregation and genomic stability by preventing the formation of incorrect KT-MT attachments [20, 21]. Studies in *D. melanogaster* culture cells showed that the single *clasp* orthologue in this organism is required for the poleward translocation of MT subunits within KT-MTs [3]. To dissect the functional significance of the interaction between CLASPs and CENP-E in this process, we used pulses from a 405 nm laser to photoactivate GFP-α-tubulin stably

expressed in human U2OS cells and measured the velocity at which the fluorescent mark activated in the proximity of chromosomes approached the pole. Consistent with previous reports [22], in control cells at late prometaphase/metaphase the fluorescent mark approached the pole with a mean velocity of 0.53 ± 0.18 μm/min (Figure 3a, Table 1 and Movie S1), with cells entering anaphase with normal kinetics after photoactivation (data not shown). In contrast, after RNAi depletion of ~90% of CLASP1 or both CLASPs (Figure S2), the fluorescent mark approached the pole at 0.36 ± 0.09 μm/min and 0.26± 0.10 μm/min, respectively (Figure 3b, Table 1 and Movie S1). Depletion of ~80% of CENP-E by RNAi (Sup. Figure 2d) phenocopies the simultaneous depletion of both CLASPs, with the fluorescent mark approaching the pole at 0.27 ± 0.11 μm/min (Figure 3c, Table 1 and Movie S1). In a small subset of experiments we were successful in marking both half-spindles and noted a similar reduction in the rates that fluorescent marks on opposing KT-MTs move apart after CLASPs or CENP-E RNAi in comparison with controls (Table 1). Altogether, these results suggest that flux rates in human cells are sensitive to the KT levels of CLASP1 and CLASP2, which are largely determined by CENP-E. Curiously, loss of function of the single *clasp* orthologue in *Drosophila* causes bipolar spindles to gradually collapse into monopolar spindles due to continuous depolymerization of MTs at their minus-ends, while tubulin subunit incorporation at the plus-ends is attenuated [3, 23]. This scenario is somewhat different from our knock-down of CLASPs (or CENP-E) in human cells, where spindles are 20-30% shorter than control cells in prometaphase or metaphase (n Luciferase RNAi=29; n CLASPs RNAi=28; n CENP-E RNAi=13; $p<0.001$, t-test), but only rarely form monopolar spindles (Figure 3d; [24] and our unpublished observations). However, anti-CLASP1 antibody injections in

HeLa cells did cause the formation of monopolar spindles [2], suggesting that some residual function of CLASPs after RNAi is still sufficient to prevent the full collapse of the spindle, while allowing some poleward MT flux.

We also determined how CLASPs and CENP-E affect KT-MT turnover by measuring fluorescence loss on the photoactivated area over time, after background subtraction and photobleaching correction, and fitting the results to a double exponential curve [19-21, 25]. The fast-decay component has been interpreted to represent non-KT-MTs that rapidly lose their activated fluorescence, while the slower-decay component likely corresponds to the more stable KT-MTs in which the activated fluorescence is more persistent (Figure 3e). Surprisingly, the calculated half-time turnover for KT-MTs in cells depleted for CLASPs or CENP-E was significantly higher (respectively 396.5 ± 48 sec; n=8, $p<0.001$, and 317.3 ± 35.2 sec; n=13, $p<0.025$) than in control cells (155.2±13.9 sec, n=14) (Figure 3e and f and Figure S2), suggesting increased KT-MT stability.. Previous studies in mammalian cells lacking CENP-E or that were microinjected with function-blocking antibodies have shown 23-50% reduction in MT binding at KTs, which was interpreted as CENP-E being required to stabilize KT-MT attachments [26, 27]. However, depletion of CENP-E or CLASPs in HeLa cells did not prevent the formation of cold-stable KT-MTs (Figure S7), indicating that despite of a reduction in the number of KT-MTs, these are actually more stably attached, possibly through point contacts with core KMN components [28], but the capacity to recruit new MTs might be impaired. Importantly, the half-time turnover observed for non-KT-MTs in control (16 ± 1.2 sec), CLASPs-depleted (11.9±0.9 sec) and CENP-E-depleted cells (14.6±1.2 sec) was similar, indicating that the contribution of these proteins to non-KT-

MT turnover is minor. Thus, CENP-E-mediated targeting of CLASPs to KTs renders attached MTs to exchange more rapidly and overall become less stable. Interestingly, both CLASPs and CENP-E levels at KTs decrease as cells progress from prometaphase to anaphase [2, 4, 29], consistent with the observation that KT-MTs become less dynamic at anaphase onset [19]. CLASPs may render KT-MTs less stable by recruiting the kinesin-13 MT depolymerase Kif2b to KTs, thereby promoting high MT turnover as cells progress into metaphase [21, 30]. Alternatively, the affinity of CLASPs to MTs may decrease when cells enter mitosis, altering the balance with MT depolymerases and favoring KT-MT destabilization. Interestingly, it has recently been reported that TOGp, a member of a widely conserved protein family commonly viewed as MT stabilizers, acts to destabilize spindle MTs during mitosis [31]

Depletion of Kif2a by RNAi in U2OS cells leads to the formation of monopolar spindles and bipolarity can be rescued with treatments that either disrupt the formation of KT-MTs or renders them less dynamic [21, 32]. In order to investigate whether CLASPs and CENP-E at KTs work in concert in the same molecular pathway required for spindle architecture we compared the efficiency of bipolar spindle formation after co-depleting CLASPs or CENP-E with Kif2a by RNAi (Figure S8). CLASP1 or double CLASPs depletion in U2OS cells is sufficient to rescue spindle bipolarity in ~80% of Kif2a-deficient cells while maintaining KT-MTs (Figure S8 and our unpublished observations). This is likely to be due to a relatively low contribution of CLASP2 during mitosis in U2OS cells, when compared to HeLa cells [24]. Interestingly, a functional cooperation between CLASP and the kinesin-13 protein KLP10A has been previously observed in *Drosophila* S2 cells [33, 34], suggesting evolutionary conservation of spindle architecture

in both systems. Finally, CENP-E depletion rescued spindle bipolarity in Kif2a-deficient cells in 85% of the cases (Figure S8), confirming that CLASPs and CENP-E at KTs work in the same pathway involved in spindle formation and maintenance.

Based on *in vitro* studies it has been proposed that CENP-E tethers KTs to dynamic MTs, independently of its ATPase activity [35]. Based on our functional data, this property of CENP-E can be explained *in vivo* by a novel motor-independent role in targeting CLASPs to KTs, thereby contributing to establish/maintain functional KT-MT attachments. Noteworthy, perturbation of CLASPs function does not give persistent mono-oriented chromosomes like many cells following CENP-E inibition [5, 17, 26, 36]. This suggests that there are some unique activities of CENP-E that are not fulfilled by CLASPs. In this context, we propose that CENP-E integrates at least two activities. One is to power (through its kinesin motor activity) chromosome alignment [36], a function that is somewhat independent of CLASPs. The second function of CENP-E is to recruit CLASPs to KTs to functionally modulate KT-MT dynamics, which explains why KT-MT flux and turnover change if either CLASPs or CENP-E are lost. On the basis of the more complex spindle phenotype associated with CLASPs depletion in HeLa cells there might be other CLASPs-interacting proteins involved in centriole and spindle function found in this study, which do not interact with CENP-E (our unpublished observations). Finally, the results presented in this paper challenge current models for how CENP-E communicates with the spindle-assembly checkpoint (SAC) [37-39]. According to these models, CENP-E has been seen to be important for the capture and stabilization of MTs at KTs, thereby contributing to SAC silencing. In light of the new data presented in this paper supporting that CENP-E promotes destabilization rather than stabilization of MT

attachments, alternative models must be put forward. An attractive one might involve the participation of CENP-E in destabilizing erroneous KT-MT attachments under control of Aurora B [20], while antagonizing the MT-stabilizing role of BubR1 [40, 41]. Since Aurora B controls the targeting of BubR1, CENP-E and Kif2b to KTs [21, 42] it is a likely possibility that CLASPs are also important players under regulation by this pathway to make mitosis error-free.

References

1. Cheeseman, I.M., and Desai, A. (2008). Molecular architecture of the kinetochore-microtubule interface. Nat Rev Mol Cell Biol *9*, 33-46.
2. Maiato, H., Fairley, E.A., Rieder, C.L., Swedlow, J.R., Sunkel, C.E., and Earnshaw, W.C. (2003). Human CLASP1 is an outer kinetochore component that regulates spindle microtubule dynamics. Cell *113*, 891-904.
3. Maiato, H., Khodjakov, A., and Rieder, C.L. (2005). Drosophila CLASP is required for the incorporation of microtubule subunits into fluxing kinetochore fibres. Nat Cell Biol *7*, 42-47.
4. Pereira, A.L., Pereira, A.J., Maia, A.R., Drabek, K., Sayas, C.L., Hergert, P.J., Lince-Faria, M., Matos, I., Duque, C., Stepanova, T., et al. (2006). Mammalian CLASP1 and CLASP2 cooperate to ensure mitotic fidelity by regulating spindle and kinetochore function. Mol Biol Cell *17*, 4526-4542.
5. Wood, K.W., Sakowicz, R., Goldstein, L.S., and Cleveland, D.W. (1997). CENP-E is a plus end-directed kinetochore motor required for metaphase chromosome alignment. Cell *91*, 357-366.
6. Cheeseman, I.M., and Desai, A. (2005). A combined approach for the localization and tandem affinity purification of protein complexes from metazoans. Sci STKE *2005*, pl1.
7. Akhmanova, A., Hoogenraad, C.C., Drabek, K., Stepanova, T., Dortland, B., Verkerk, T., Vermeulen, W., Burgering, B.M., De Zeeuw, C.I., Grosveld, F., et al. (2001). Clasps are CLIP-115 and -170 associating proteins involved in the regional regulation of microtubule dynamics in motile fibroblasts. Cell *104*, 923-935.
8. Lansbergen, G., Grigoriev, I., Mimori-Kiyosue, Y., Ohtsuka, T., Higa, S., Kitajima, I., Demmers, J., Galjart, N., Houtsmuller, A.B., Grosveld, F., et al. (2006). CLASPs attach microtubule plus ends to the cell cortex through a complex with LL5beta. Dev Cell *11*, 21-32.
9. Efimov, A., Kharitonov, A., Efimova, N., Loncarek, J., Miller, P.M., Andreyeva, N., Gleeson, P., Galjart, N., Maia, A.R., McLeod, I.X., et al. (2007). Asymmetric CLASP-dependent nucleation of noncentrosomal microtubules at the trans-Golgi network. Dev Cell *12*, 917-930.
10. Hannak, E., and Heald, R. (2006). Xorbit/CLASP links dynamic microtubules to chromosomes in the Xenopus meiotic spindle. J Cell Biol *172*, 19-25.
11. Delgehyr, N., Sillibourne, J., and Bornens, M. (2005). Microtubule nucleation and anchoring at the centrosome are independent processes linked by ninein function. J Cell Sci *118*, 1565-1575.
12. Kleylein-Sohn, J., Westendorf, J., Le Clech, M., Habedanck, R., Stierhof, Y.D., and Nigg, E.A. (2007). Plk4-induced centriole biogenesis in human cells. Dev Cell *13*, 190-202.
13. Drewes, G., Ebneth, A., Preuss, U., Mandelkow, E.M., and Mandelkow, E. (1997). MARK, a novel family of protein kinases that phosphorylate microtubule-associated proteins and trigger microtubule disruption. Cell *89*, 297-308.

14. Cooke, C.A., Schaar, B., Yen, T.J., and Earnshaw, W.C. (1997). Localization of CENP-E in the fibrous corona and outer plate of mammalian kinetochores from prometaphase through anaphase. Chromosoma *106*, 446-455.
15. Cheeseman, I.M., MacLeod, I., Yates, J.R., 3rd, Oegema, K., and Desai, A. (2005). The CENP-F-like proteins HCP-1 and HCP-2 target CLASP to kinetochores to mediate chromosome segregation. Curr Biol *15*, 771-777.
16. Bomont, P., Maddox, P., Shah, J.V., Desai, A.B., and Cleveland, D.W. (2005). Unstable microtubule capture at kinetochores depleted of the centromere-associated protein CENP-F. Embo J *24*, 3927-3939.
17. Schaar, B.T., Chan, G.K., Maddox, P., Salmon, E.D., and Yen, T.J. (1997). CENP-E function at kinetochores is essential for chromosome alignment. J Cell Biol *139*, 1373-1382.
18. Henderson, M.C., Shaw, Y.J., Wang, H., Han, H., Hurley, L.H., Flynn, G., Dorr, R.T., and Von Hoff, D.D. (2009). UA62784, a novel inhibitor of centromere protein E kinesin-like protein. Mol Cancer Ther *8*, 36-44.
19. Zhai, Y., Kronebusch, P.J., and Borisy, G.G. (1995). Kinetochore microtubule dynamics and the metaphase-anaphase transition. J Cell Biol *131*, 721-734.
20. Cimini, D., Wan, X., Hirel, C.B., and Salmon, E.D. (2006). Aurora kinase promotes turnover of kinetochore microtubules to reduce chromosome segregation errors. Curr Biol *16*, 1711-1718.
21. Bakhoum, S.F., Thompson, S.L., Manning, A.L., and Compton, D.A. (2009). Genome stability is ensured by temporal control of kinetochore-microtubule dynamics. Nat Cell Biol *11*, 27-35.
22. Ganem, N.J., Upton, K., and Compton, D.A. (2005). Efficient mitosis in human cells lacking poleward microtubule flux. Curr Biol *15*, 1827-1832.
23. Maiato, H., Sampaio, P., Lemos, C.L., Findlay, J., Carmena, M., Earnshaw, W.C., and Sunkel, C.E. (2002). MAST/Orbit has a role in microtubule-kinetochore attachment and is essential for chromosome alignment and maintenance of spindle bipolarity. J Cell Biol *157*, 749-760.
24. Mimori-Kiyosue, Y., Grigoriev, I., Sasaki, H., Matsui, C., Akhmanova, A., Tsukita, S., and Vorobjev, I. (2006). Mammalian CLASPs are required for mitotic spindle organization and kinetochore alignment. Genes Cells *11*, 845-857.
25. DeLuca, J.G., Gall, W.E., Ciferri, C., Cimini, D., Musacchio, A., and Salmon, E.D. (2006). Kinetochore microtubule dynamics and attachment stability are regulated by Hec1. Cell *127*, 969-982.
26. McEwen, B.F., Chan, G.K., Zubrowski, B., Savoian, M.S., Sauer, M.T., and Yen, T.J. (2001). CENP-E is essential for reliable bioriented spindle attachment, but chromosome alignment can be achieved via redundant mechanisms in mammalian cells. Mol Biol Cell *12*, 2776-2789.
27. Putkey, F.R., Cramer, T., Morphew, M.K., Silk, A.D., Johnson, R.S., McIntosh, J.R., and Cleveland, D.W. (2002). Unstable kinetochore-microtubule capture and chromosomal instability following deletion of CENP-E. Dev Cell *3*, 351-365.
28. Cheeseman, I.M., Chappie, J.S., Wilson-Kubalek, E.M., and Desai, A. (2006). The conserved KMN network constitutes the core microtubule-binding site of the kinetochore. Cell *127*, 983-997.

29. Hoffman, D.B., Pearson, C.G., Yen, T.J., Howell, B.J., and Salmon, E.D. (2001). Microtubule-dependent changes in assembly of microtubule motor proteins and mitotic spindle checkpoint proteins at PtK1 kinetochores. Mol Biol Cell *12*, 1995-2009.
30. Manning, A.L., Ganem, N.J., Bakhoum, S.F., Wagenbach, M., Wordeman, L., and Compton, D.A. (2007). The kinesin-13 proteins Kif2a, Kif2b, and Kif2c/MCAK have distinct roles during mitosis in human cells. Mol Biol Cell *18*, 2970-2979.
31. Cassimeris, L., Becker, B., and Carney, B. (2009). TOGp regulates microtubule assembly and density during mitosis and contributes to chromosome directional instability. Cell Motil Cytoskeleton *66*, 535-545.
32. Ganem, N.J., and Compton, D.A. (2004). The KinI kinesin Kif2a is required for bipolar spindle assembly through a functional relationship with MCAK. J Cell Biol *166*, 473-478.
33. Laycock, J.E., Savoian, M.S., and Glover, D.M. (2006). Antagonistic activities of Klp10A and Orbit regulate spindle length, bipolarity and function in vivo. J Cell Sci *119*, 2354-2361.
34. Buster, D.W., Zhang, D., and Sharp, D.J. (2007). Poleward tubulin flux in spindles: regulation and function in mitotic cells. Mol Biol Cell *18*, 3094-3104.
35. Lombillo, V.A., Nislow, C., Yen, T.J., Gelfand, V.I., and McIntosh, J.R. (1995). Antibodies to the kinesin motor domain and CENP-E inhibit microtubule depolymerization-dependent motion of chromosomes in vitro. J Cell Biol *128*, 107-115.
36. Kapoor, T.M., Lampson, M.A., Hergert, P., Cameron, L., Cimini, D., Salmon, E.D., McEwen, B.F., and Khodjakov, A. (2006). Chromosomes can congress to the metaphase plate before biorientation. Science *311*, 388-391.
37. Abrieu, A., Kahana, J.A., Wood, K.W., and Cleveland, D.W. (2000). CENP-E as an essential component of the mitotic checkpoint in vitro. Cell *102*, 817-826.
38. Mao, Y., Desai, A., and Cleveland, D.W. (2005). Microtubule capture by CENP-E silences BubR1-dependent mitotic checkpoint signaling. J Cell Biol *170*, 873-880.
39. Yao, X., Abrieu, A., Zheng, Y., Sullivan, K.F., and Cleveland, D.W. (2000). CENP-E forms a link between attachment of spindle microtubules to kinetochores and the mitotic checkpoint. Nat Cell Biol *2*, 484-491.
40. Lampson, M.A., and Kapoor, T.M. (2005). The human mitotic checkpoint protein BubR1 regulates chromosome-spindle attachments. Nat Cell Biol *7*, 93-98.
41. Maia, A.F., Lopes, C.S., and Sunkel, C.E. (2007). BubR1 and CENP-E have antagonistic effects upon the stability of microtubule-kinetochore attachments in Drosophila S2 cell mitosis. Cell Cycle *6*, 1367-1378.
42. Ditchfield, C., Johnson, V.L., Tighe, A., Ellston, R., Haworth, C., Johnson, T., Mortlock, A., Keen, N., and Taylor, S.S. (2003). Aurora B couples chromosome alignment with anaphase by targeting BubR1, Mad2, and Cenp-E to kinetochores. J Cell Biol *161*, 267-280.
43. Poser, I., Sarov, M., Hutchins, J.R., Heriche, J.K., Toyoda, Y., Pozniakovsky, A., Weigl, D., Nitzsche, A., Hegemann, B., Bird, A.W., et al. (2008). BAC

TransgeneOmics: a high-throughput method for exploration of protein function in mammals. Nat Methods *5*, 409-415.

44. Harborth, J., Elbashir, S.M., Bechert, K., Tuschl, T., and Weber, K. (2001). Identification of essential genes in cultured mammalian cells using small interfering RNAs. J Cell Sci *114*, 4557-4565.
45. DeLuca, J.G., Moree, B., Hickey, J.M., Kilmartin, J.V., and Salmon, E.D. (2002). hNuf2 inhibition blocks stable kinetochore-microtubule attachment and induces mitotic cell death in HeLa cells. J Cell Biol *159*, 549-555.
46. Mimori-Kiyosue, Y., Grigoriev, I., Lansbergen, G., Sasaki, H., Matsui, C., Severin, F., Galjart, N., Grosveld, F., Vorobjev, I., Tsukita, S., et al. (2005). CLASP1 and CLASP2 bind to EB1 and regulate microtubule plus-end dynamics at the cell cortex. J Cell Biol *168*, 141-153.
47. Link, A.J., Eng, J., Schieltz, D.M., Carmack, E., Mize, G.J., Morris, D.R., Garvik, B.M., and Yates, J.R., 3rd (1999). Direct analysis of protein complexes using mass spectrometry. Nat Biotechnol *17*, 676-682.

Acknowledgements

We thank I. Cheeseman for guidance and providing reagents for LAP purifications, A. J. Pereira and S. Bakhoum for the development of Matlab routines used in this paper and advice on the quantification of microtubule dynamics parameters, P. Sampaio for help with photoactivation and A. Akhmanova, T. Yen and W. Earnshaw for the generous gift of reagents. S.M., A.R.R.P., and A.L.P hold fellowships from Fundação para a Ciência e a Tecnologia (FCT) of Portugal (SFRH/BPD/26780/2006; SFRH/BD/32976/2006; SFRH/BD/25084/2005**).** Work in the lab of D.A.C. is supported by National Institutes of Health grant GM51542. Work in the laboratory of H.M. is supported by grants PTDC/BIA-BCM/66106/2006 and PTDC/SAU-OBD/66113/2006 from FCT and the Gulbenkian Programme on the Frontiers in Life Sciences.

Experimental Procedures

Cell culture, RNAi, Drug treatments, Transfections and Western Blot Analysis.

Human HeLa cells, HeLa LAP-CLASP1 [4], HeLa CENP-E-GFP [43] and U2OS-PA-GFP-α-tubulin cells [22] were grown in DMEM at 37°C in the presence of 5% CO_2 and supplemented with 10% fetal bovine serum (FBS) and antibiotics. Human CLASP1, CLASP2, CENP-E, Kif2a and Nuf2 levels were reduced using specific siRNA oligonucleotides as previously described [24, 32, 44, 45] (Manning et al., submitted). Phenotypes were analyzed and quantified 48 h and 72 h after RNAi treatment and protein depletion was monitored by western blot using the following antibodies: rabbit anti-CLASP1 1:1000 [46]; rat anti-CLASP1 1:200, rabbit anti-CENP-E 1:500 (Santa Cruz); anti-Kif2a [32]; anti-Eg5 (Manning et al., submitted) and mouse anti-α-tubulin 1:2000 (Sigma). HRP-conjugated secondary antibodies (Amersham) were visualized using the ECL system (Pierce). To enrich HeLa LAP-CLASP1 or HeLa CENP-E-GFP cell cultures for mitotic cells for mass spectrometry and immunoprecipitation analyses, 100 ng/mL or 5ng/mL nocodazole, respectively, was added to the media for 16 or 18 h before harvesting. For inhibition of CENP-E ATPase activity, 100 nM of UA62784 was added to the media for 12 h before the analysis [18]. For photobleaching correction in the MT half time turnover experiments, control cells were treated with 5 μm Taxol 10 min before starting imaging. Transfection of HeLa cells with GFP-CENP-E NΔ803 was performed as described [2] and analysed 48 h after transfection. Wild-type and clasp2 KO MEFs were grown as previously described [4].

Immunofluorescence

HeLa or U20S cells were processed for immunofluorescence as described previously [2, 32]. Primary antibodies used were: rabbit anti-CLASP1 1:300 [2]; sheep anti-CENP-E 1:500 (gift from W. Earnshaw, University of Edinburgh, Edinburgh, UK); rat anti-CLASP1 1:100; rat anti-CLASP2 1:100, rabbit anti-CENP-E 1:300 (Santa Cruz); human anti-ACA 1:1000 (gift from W. Earnshaw) and mouse anti-α-tubulin 1:2000 (Sigma). Immunofluorescence on chromosome spreads was performed as described [2]. Secondary antibodies used were Alexa 488, 568 and 647 1:2000 (Invitrogen, Molecular Probes) and

DNA was counterstained with DAPI (1 μg/ml). For cold induced MT-depolymerisation experiments, HeLa cells were incubated 15 min on ice and 1 min with 0.2% Triton X-100 in PHEM buffer (60 mM Pipes, 25 mM Hepes, 10 mM EGTA, 2 mM $MgCl_2$). After a 30 min fixation in 4% paraformaldehyde in PHEM buffer followed by a 5 min methanol post-fixation, cells were processed for immunofluorescence as described above.

Mass spectrometry and Immunoprecipitation

Native protein extracts from HeLa LAP-CLASP1 [4] or HeLa CENP-E-GFP [43] cell cultures enriched for mitotic cells by nocodazole treatment were prepared for mass spectrometry analysis as described [6, 47]. The presented list of CLASP1-interacting proteins was filtered for known common contaminants in LAP-purifications. Immunoprecipitation experiments were performed with aliquots of native protein extracts (3 mg of total protein in a total volume of 500 μl of IP buffer: 150 mM Kcl, 75mM Hepes p.H 7.5, 1.5 mM EGTA, 1.5 mM $MgCl_2$, 10 % glycerol, 0.1 % NP40, protease inhibitors) prepared from HeLa LAP-CLASP1 or HeLa CENP-E-GFP cell cultures enriched for mitotic cells by incubation with nocodazole. Protein extracts were incubated with the precipitating antibody at 4 ^{o}C for 4 h on a rotating platform. Precipitating primary antibodies used were: rabbit anti-GFP 1:100 and rabbit anti-GFP pre-immunization serum (GFP-PI) 1:100. These extracts were then incubated with 40 μl of protein A-Sepharose for 2 h at 4 ^{o}C on a rotating platform. Samples were centrifuged, the supernatant was retained as unbound sample and the pelleted beads washed 3 times with washing buffer (IP buffer with 250 mM KCl). Precipitated proteins were removed from the beads by boiling 5 min in SDS sample buffer and subjected to electrophoresis followed by western blot analysis with the appropriate antibody: rabbit anti-GFP 1:1000; rabbit anti-CENP-E 1:100 (Santa Cruz); anti-LL5β 1:2000 (gift from Anna Akhmanova, Erasmus Medical Center, Rotterdam, The Netherlands); anti-α-tubulin 1:2000 (Sigma) and rabbit anti-CLASP1 1:1000 [46].

Fluorescence quantification at KTs

Protein accumulation at KTs of HeLa cells prepared for chromosome spreads and immunostained with rat anti-CLASP1 or rat anti-CLASP2, rabbit anti-CENP-E and

human anti-ACA, was measured for individual KTs by quantification of the pixel gray levels of the focused z-plane within a region of interest (ROI). Background was measured outside the ROI and was subtracted to the measured fluorescent intensity inside the ROI. Results were normalized against a constitutive KT marker (ACA) using a custom routine written in Matlab.

GFP-α-tubulin photoactivation analysis

For photoactivaton studies, mitotic human U2OS cells stably expressing photoactivatable GFP-α-tubulin [22] were identified by DIC microscopy and after acquisition of a pre-activation frame, 2x0.8 sec pulses from a 405-nm laser were used to activate GFP-α-tubulin in one or two areas of ~7 μm^2 inside the spindle. Imaging was performed with a Leica SP2 spectral confocal with a 63x/1.4 NA objective lens with an additional zoom of 7x and images were acquired every 3 sec in the first 4 min and subsequently every 30 sec. For MT poleward flux experiments the quantification of fluorescence intensity of the activated areas and the quantification of flux rates were performed as described [22]. Quantification of MT half time turnover was performed as previously described [19-21, 25] where the background-subtracted fluorescence values of an activated area were corrected for photobleaching by determining the fluorescence loss in activated spindles from taxol-treated cells. The fluorescent values were normalized to the first time-point following photoactivation and averaged from different cells for each time-point. The kinetics of fluorescence loss after activation were fit to a double exponential curve and the regression analysis was performed as described [19-21, 25] using the Origin 6 software (Originlab, MA).

Spindle structure analysis

Spindle length from prometaphase or metaphase HeLa cells were calculated with ImageJ software by measuring the distance between spindle poles in 3D. CLASP1 or CENP-E staining at the poles was used as reference. Assays for the analysis of bipolar spindle formation after siRNA depletion of the indicated proteins was performed as described [32].

Figure Legends

Figure 1 – Human CLASP1 interacts with CENP-E. (A) Mass spectrometry analysis of affinity purified GFP-(LAP)-CLASP1 and CENP-E-GFP identifies novel protein interactions. Polypeptides identified (Prey) and the percentages of the relative sequence coverage are indicated. A complete list of the polypeptides identified during this analysis is given in Table S1. **(B)** Anti-GFP Immunoprecipitation from mitotic enriched HeLa cells stably expressing GFP-(LAP)-CLASP1 or CENP-E-GFP. Native protein extracts (Load) obtained from the indicated cell lines, unbound proteins (Unbd) and immunoprecipitations (IP) were subjected to western blot analysis with the indicated antibody. Immunoprecipitations were blotted for LL5β and α-tubulin as positive and negative controls. Immunoprecipitations performed using anti-GFP pre-immunization serum (GFP-PI) as precipitating antibody were analyzed by western blotting with rabbit anti-CLASP1 antibody. Quantification of CENP-E levels in the GFP-CLASP1 immunoprecipitation revealed +131% increase relative to control. Quantification of CLASP1 levels in the CENP-E-GFP immunoprecipitation revealed +135% increase relative to control.

Figure 2 – CENP-E targets CLASP1 to KTs in a Motor-independent manner. (A-C) Interdependency analysis of CLASP1 and CENP-E localization. HeLa cells treated with the indicated specific siRNA were prepared for chromosomes spreads in the presence of 10 μM nocodazole to fully depolymerize MTs. Following fixation, cells were stained for endogenous CLASP1 and CENP-E. ACA was used as an inner-KT marker and DNA was

stained with DAPI. **(D and E)** The dependency of CLASP1 KT targeting from the motor domain of CENP-E was tested in HeLa cells transfected with a construct over-expressing a dominant negative motor-less GFP-CENP-E (GFP-CENP-E NΔ803) (D), or HeLa cells treated with UA62784 (E), an inhibitor of CENP-E ATPase activity. Cells were prepared for chromosomes spreads, fixed and stained for CLASP1 (D) or CLASP1 and CENP-E (E). For each cell, a magnification of an area containing KTs (colored as indicated) is shown in the smaller panels. Arrowheads indicate centrosomes. Scale bar= 5 μm. **(F)** Quantification of CLASP1/ACA KT fluorescence ratio in control (A), CENP-E RNAi (C), cells transfected with GFP-CENP-E NΔ803 (D) or treated with UA62784 (E).

Figure 3 – CENP-E targeting of CLASP1 to KTs is required to sustain normal KT-MT dynamics. (A-C) Human U2OS cells in late prometaphase/metaphase depleted for CLASPs or CENP-E display a significant reduction of KT MT poleward flux. Metaphase cells were identified by DIC and imaged (Pre) while flourescence images were captured before (Pre) and at various times (indicated in seconds) after photoactivation of GFP-α-tubulin with pulses from a 405 nm laser in one or two areas of the spindle (green rectangles). Line scans represent the relative fluorescence intensity of individual KT-MTs in a defined area (red rectangle) of the fluorescence images. Lines indicate the position of peak fluorescence intensity and flux rates were determined by plotting the position of peak fluorescence intensity as a function of time. Red circles indicate the position of spindle poles. Flux values correspond to the mean ± standard deviation. Scale bar= 1 μm. **(D)** Cells deficient for CENP-E or CLASPs show shorter spindles (PM=Prometaphase;

M=Metaphase). Data represent the mean and error bars correspond to standard deviation. **(E)** Cells depleted for CENP-E or CLASPs show a significantly higher KT MT half time turnover. Normalized fluorescence intensity over time after photoactivation of U20S cells (in late PM/M) following treatment with the indicated siRNA. Data represent the mean and error bars correspond to standard error after background subtraction and photobleaching correction. **(F)** Calculated MT half time turnover for U2OS cells in (E). Data represent the mean and error bars correspond to standard error.

A

Bait	Prey	% Sequence Coverage	Size (kDa)
GFP CLASP1	CLASP1	51	169
	CLIP-170	43	156
	GCC185	42	185
	Astrin	29	134
	CENP-J	16	153
	MARK2	13	83
	LL5β	8	136
	CENP-E	7	312
	Ninein	4	243
CENP-E GFP	CENP-E	41	312
	CLASP1	12	169
	CLASP2	7	165
	PRC1	4	72

B

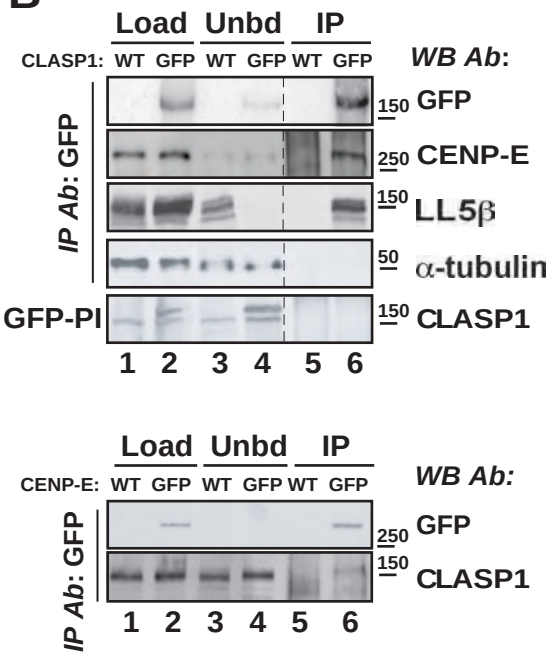

Figure 1 - Maffini et al.,

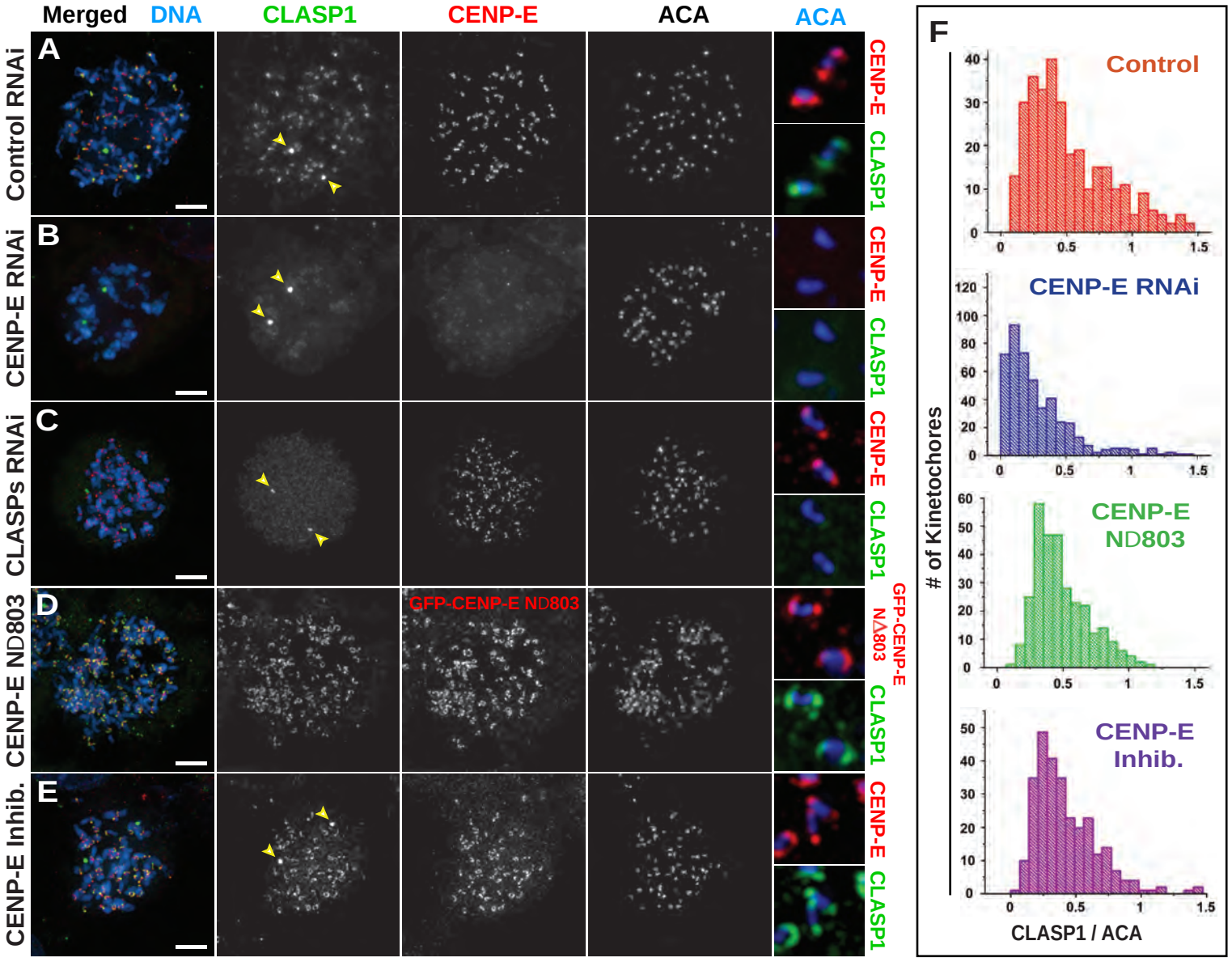

Figure 2 - Maffini et al.,

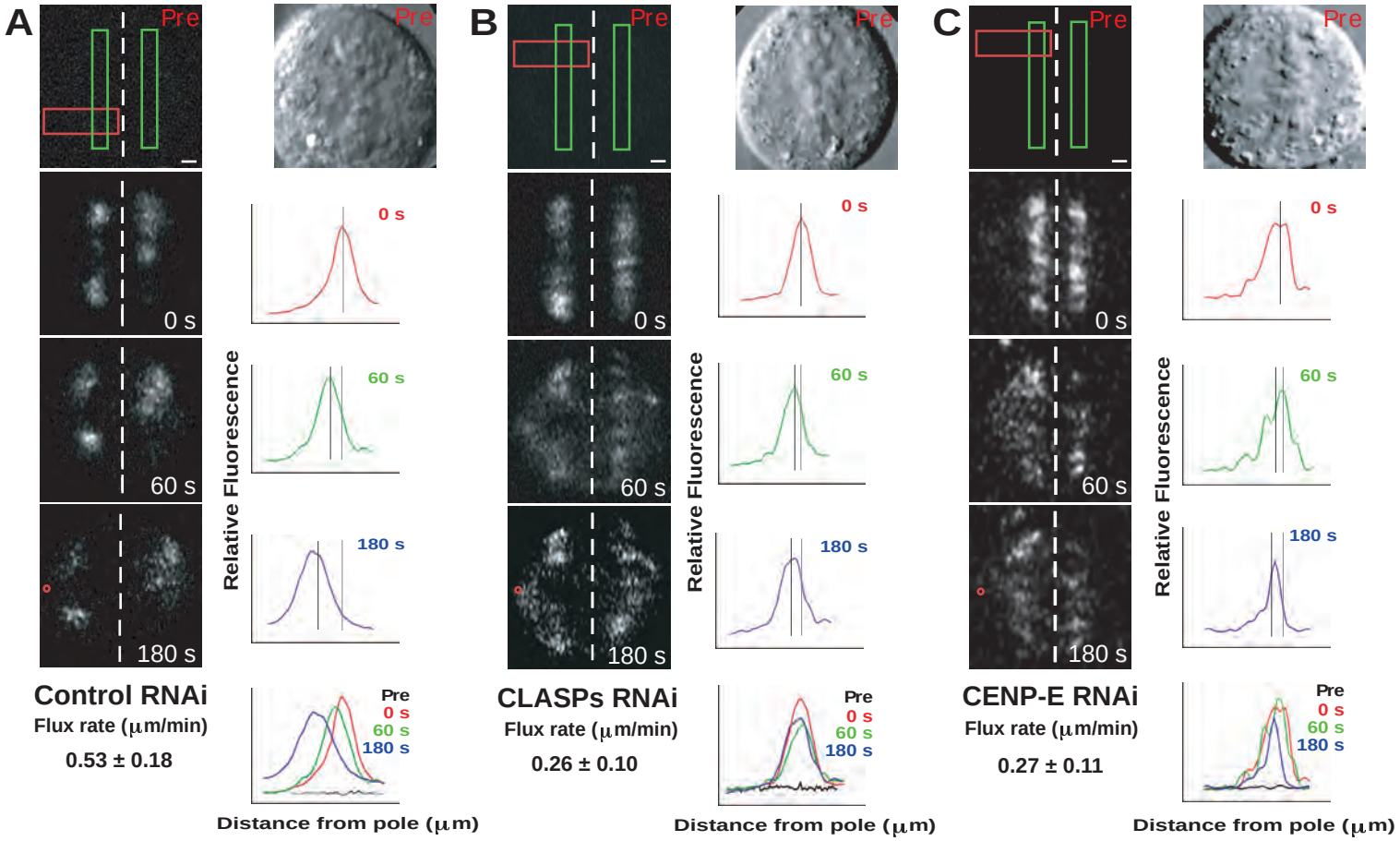

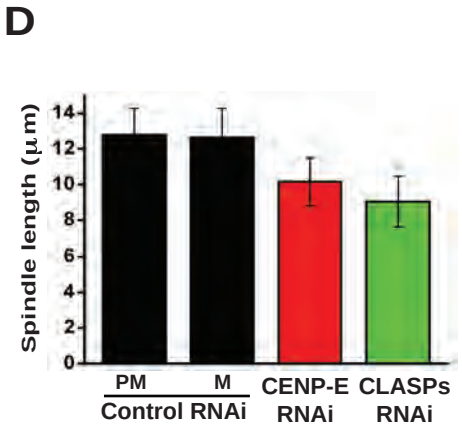

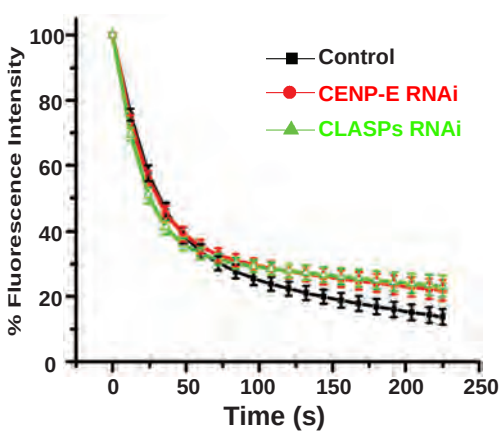

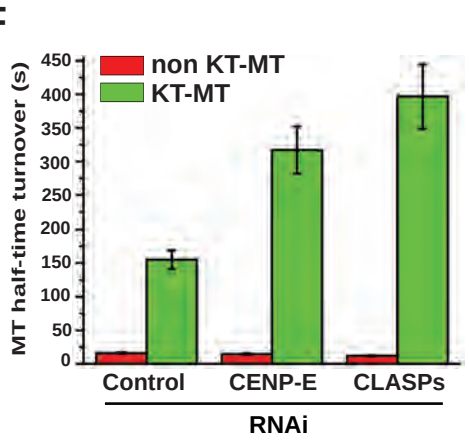

Figure 3 - Maffini et al.